A coalescence model for SonoVue

Michiel Postema, Sascha Hilgenfeldt, Charles T Lancée, Philippe Marmottant, Annemieke van Wamel

Contribution to Bracco SonoVue™ modeling contest

by

Michiel Postema*
Sascha Hilgenfeldt†
Charles T. Lancée‡
Philippe Marmottant§
Annemieke van Wamel‡¶

* Institute for Medical Engineering, Ruhr-University Bochum, Bochum, Germany
† Engineering Sciences & Applied Mathematics and Dept. of Mechanical Engineering, Northwestern University, Evanston, IL, USA
‡ Department of Experimental Echocardiography, Thoraxcentre, Erasmus MC, Rotterdam, The Netherlands
§ Laboratoire de Spectrométrie Physique, CNRS – Université Joseph Fourier, Saint Martin d' Hères, France
¶ Interuniversity Cardiology Institute of the Netherlands, Utrecht, The Netherlands

Correspondence to M. Postema: postema@ieee.org

A coalescence model for SonoVue™

Michiel Postema*, Sascha Hilgenfeldt†, Charles T. Lancée‡, Philippe Marmottant§, Annemieke van Wamel‡¶

* Institute for Medical Engineering, Ruhr-University Bochum, Bochum, Germany
† Engineering Sciences & Applied Mathematics and Dept. of Mechanical Engineering, Northwestern University, Evanston, IL, USA
‡ Department of Experimental Echocardiography, Thoraxcentre, Erasmus MC, Rotterdam, The Netherlands
§ Laboratoire de Spectrométrie Physique, CNRS – Université Joseph Fourier, Saint Martin d'Hères, France
¶ Interuniversity Cardiology Institute of the Netherlands, Utrecht, The Netherlands

I. Introduction

SonoVue™ is a second generation contrast agent, consisting of SF_6 gas microbubbles encapsulated by an elastic lipid shell. It is the only agent allowed for clinical use in Europe. Predicting the dynamic behavior of ultrasound insonified SonoVue™ microbubbles has been of much clinical interest. To improve detection methods and to develop therapeutic applications, the behavior of individual microbubbles has been observed and analyzed.

Because SonoVue™ has a mean diameter of $2\,\mu$m, its resonance frequency is above $3\,$MHz. Bubbles smaller than resonant size hardly generate an acoustic response, but insonifying at higher frequencies seriously affects the penetration depth of the ultrasound. The coalescence of microbubbles might be used to increase the acoustic response from bulk agent at relatively low acoustic frequencies, without increasing the dosage. Since the strongest acoustic response is generated by bubbles above resonant size, a theoretically simple way to increase scattering from contrast agent would be to induce bubble coalescence until the bubbles reach resonant sizes.

In this paper, a method is presented to model coalescence behavior of SonoVue™ microbubbles. The *in vitro* experiments have been performed on a similar agent.

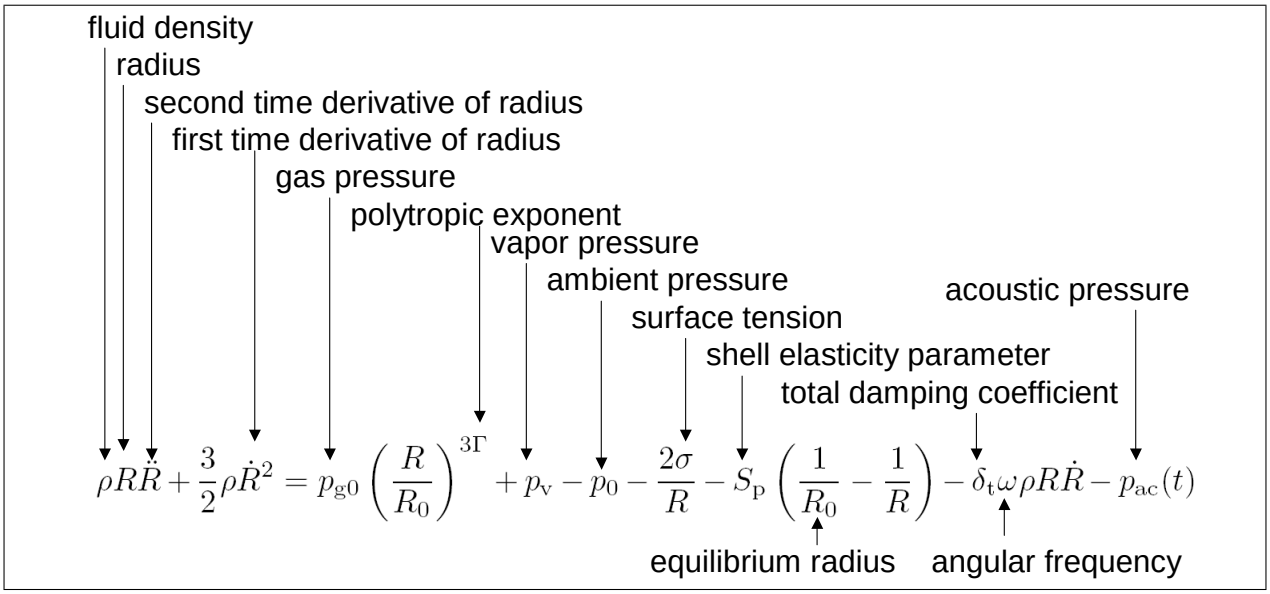

Fig. 1. Modified RPNNP equation, including the shell elasticity parameter S_p.

II. Oscillating lipid-encapsulated bubbles

Most models have been based on those for oscillating free gas bubbles. An overview of oscillating free gas bubble models was published by Vokurka [1]. Although the well-known RPNNP equation properly describes the oscillations of an individual microbubble in an ultrasonic field, it does not account for the presence of an encapsulation. De Jong introduced shell parameters to account for the presence of the shell [2], [3]. The resulting modified RPNNP equation is demonstrated in Figure 1. The effect of the internal

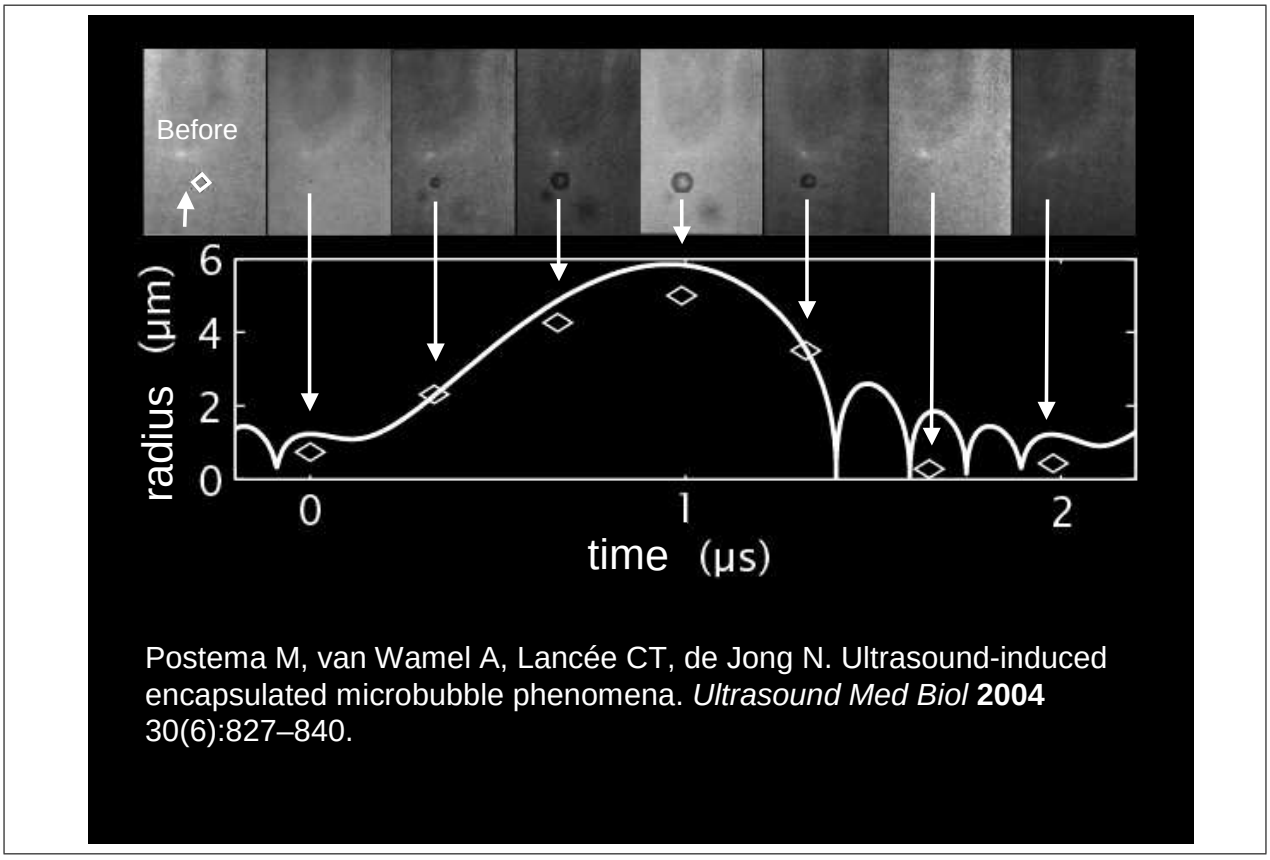

Fig. 2. Oscillating experimental contrast microbubble. The image sequence spans one ultrasonic cycle. The first frame has been captured prior to ultrasound arrival. Inter-frame times for the other frames are $0.33\,\mu$s. Each frame corresponds to a $88 \times 58\,\mu\text{m}^2$ area. Above: a $\oslash$ $1.5\,\mu$m bubble strongly oscillates (MI$= 0.67$). Below: radius–period plot of the event. The solid line represents an oscillating free gas bubble.

friction inside the shell is included in the total damping coefficient [2], [4], [5]:

$$\delta_{\text{t}} = \delta_{\text{rad}} + \delta_{\text{vis}} + \delta_{\text{th}} + \frac{S_{\text{f}}}{m\omega}, \tag{1}$$

where δ_{rad} is the damping coefficient due to reradiation, δ_{vis} is the viscous damping coefficient, δ_{th} is the thermal damping coefficient, S_{f} is the shell friction parameter, and m is the effective mass of the bubble–liquid system. Gorce *et al*. computed the shell elasticity parameter S_{p} and the shell friction parameter S_{f} for SonoVue™, based on acoustic measurements on bulk agent [6]. They found $S_{\text{p}} = 1.1\ \text{N}\,\text{m}^{-1}$ and $S_{\text{f}} = 0.27 \times 10^{-6}\ \text{kg}\,\text{s}^{-1}$, using acoustic pressures in the clinical diagnostic range. Postema *et al.* investigated phospholipid-encapsulated gas bubbles, kindly supplied by Bracco Reasearch SA, Geneva, Switzerland, that are very similar to SonoVue™ [7]. Instead of SF_6, however, the bubbles contain the heavier C_3F_8. Individual contrast agent microbubles were subjected to high-speed photography during insonification, and relative excursions were then compared to computations from De Jong's model and a modified Herring equation published by Morgan *et al.* [8], substituting the shell parameters from Gorce *et al*. It was found that at high acoustic pressures (MI> 0.6), De Jong's model gives conservative estimates for the maximal excursion, whereas Morgan's model predicts maximal excursions that are too high.

At high acoustic pressures, high-speed photographs show that the lipid-encapsulated bubbles may expand to more than ten-fold their initial surface areas during one ultrasonic cycle [9]. The shell consists of a lipid monolayer that, under the conditions of the experiments, is in a solid state. It behaves like an elastic membrane that ruptures under relatively small strain [10]. By the time of maximal expansion, therefore, the shell has ruptured, leaving newly formed clean free interfaces. As such, the elastic properties of the shell will have diminished, resulting in a maximal expansion similar to a free gas bubble. Figure 2 shows an example of an optical sequence of an insonified Bracco agent microbubble, captured during one high-MI ultrasonic cycle. Clearly, the simulated curve ($S_\mathrm{p} = 0$ N m^{-1}, $S_\mathrm{f} = 0$ kg s^{-1}) and the measured radii match [11].

For MI< 0.1, Gorce's shell parameters are presumed valid, whereas for MI> 0.6, shell parameters should be neglected. The validity of shell parameters in the regime $0.1 <$MI< 0.6 has been under investigation.

III. Lipid-encapsulated bubbles translating towards each other

In order to coalesce, bubbles have to translate towards each other. The mean approach velocity v_a of two approximately identical bubbles is given by [12], [11]:

$$v_\mathrm{a} = -\frac{\left(2\pi f p_\mathrm{ac}^-\right)^2}{27\eta}\,\rho\kappa^2\,\frac{R_0^5}{d_0^2}\,, \tag{2}$$

where f is the insonifying frequency, p_ac^- is the peak rarefactional acoustic pressure, η is the viscosity of the liquid, d_0 is the distance between the centers of the two bubbles, and κ is the compressibility of the bubble

$$\kappa = \frac{1}{\rho}\frac{\partial\rho}{\partial p}\,. \tag{3}$$

Figure 3 shows 5 image frames of two $\oslash\ 4\,\mu$m Bracco constrast microbubbles, each captured after

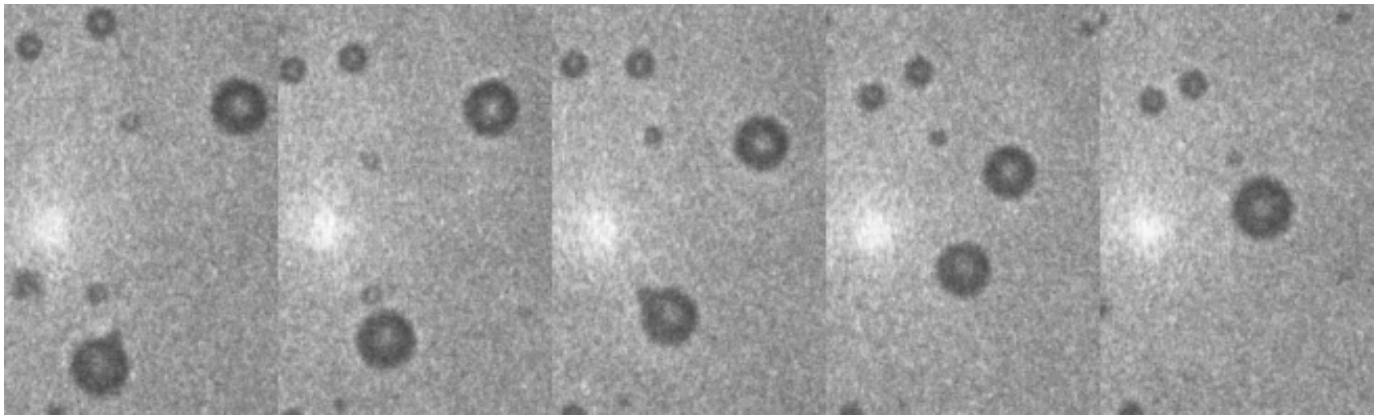

Fig. 3. The approach of two $\oslash\ 4\,\mu$m experimental contrast bubbles induced by a secondary radiation force. Each image frame corresponds to a $30 \times 20\,\mu$m^2 area. Frames are each captured after insonification by 10 cycles of 0.5 MHz ultrasound (MI$= 0.67$).

insonification by 10 cycles of 0.5 MHz ultrasound (duration $t_\mathrm{p} = 20\,\mu$s). Each image frame corresponds to a 30×20 μm^2 area. During every ultrasound burst the bubbles draw nearer to each other. For each center-to-center distance d_0 measured the mean approach velocity v_a has been computed from equation (2), taking $\kappa = 5\times10^{-6}$ m^2 N^{-1} (estimated from [2] and [12]). By combining d_0 with v_a, the theoretical distances $\Delta d_\mathrm{th} = v_\mathrm{a} t_\mathrm{p}$ have been computed. These were compared to the distance Δd_m measured from Figure 3.

TABLE I

TRAVELED DISTANCES AND MEAN VELOCITIES OF APPROACHING BUBBLES.

frame	d_0 (μm)	v_a (cm s^{-1})	Δd_th (μm)	Δd_m (μm)
a	21.2	15	3.0	3.2
b	18.0	20	4.0	3.9
c	14.1	33	6.6	6.4
d	7.7	111	> 7.7	7.7
e	0			

The results are summarized in Table I. The measured values Δd are consistent with theory. While the bubbles approach each other, their maximal sizes determine when they come into contact.

IV. FLATTENING OF THE INTERFACES AND LIPID-ENCAPSULATED MICROBUBBLE COALESCENCE

When two lipid-encapsulated gas bubbles are driven into each other, coalescence into a single bubble may result. The following stages of bubble coalescence have been identified (*cf.* Figure 4): flattening of the opposing bubble surfaces prior to contact, drainage of the interposed liquid film toward a critical minimal thickness, rupture of the liquid film, and formation of a single bubble. If the critical thickness is not reached during collision, the bubbles bounce off each other instead. Free gas bubble coalescence

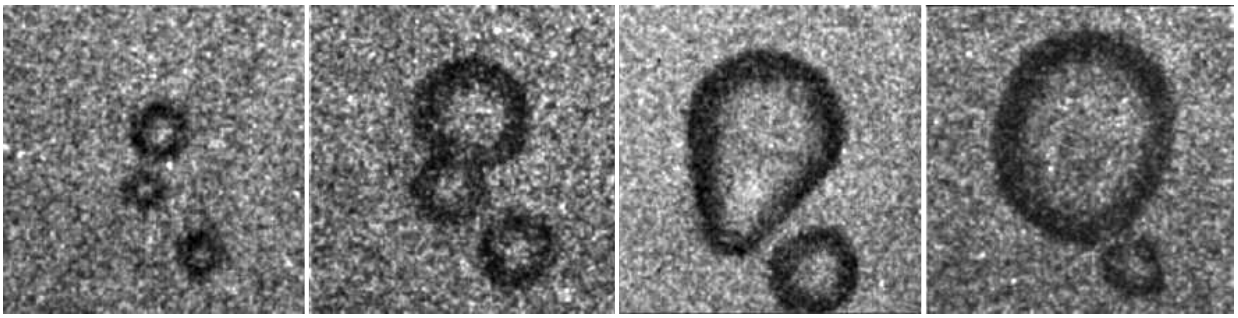

Fig. 4. Coalescing Bracco microbubbles during expansion. Interframe times are 0.33 μs. Each frame corresponds to a $21 \times 21 \mu\mathrm{m}^2$ area.

after collision has been studied extensively [13], [14], [15], [16], [17], [18]. With ultrasound contrast agents, microbubble coalescence has been observed during ultrasound insonification, when expanding microbubbles come into contact with each other [19], [9], [20]. With the aid of high-speed photography, the coalescence times of insonified Bracco microbubbles were investigated. Observed coalescence times were compared to calculated film drainage times, based on the Reynolds equation [21] for no-slip interfaces and on the drainage equation for free interfaces. It was concluded that the bubbles behaved as if they had free interfaces like free gas bubbles [9]. However, to support this conclusion, the drainage equations were also validated for expanding free gas microbubbles. Rigid-shelled contrast agent microbubbles were exposed to high-intensity ultrasound, in order to release gas, and measure the coalescence times of these free gas bubbles [22].

The Weber number for a fluid containing two bubbles with radii R_1 and R_2, respectively, is given by the inertial force relative to the surface tension force:

$$\mathrm{We} = \rho\, u^2 \Big/ \frac{\sigma}{R_\mathrm{m}} \quad , \tag{4}$$

where u is the relative approach velocity, ρ is the fluid density, σ is the surface tension, and R_m is the mean bubble radius for which holds:

$$\frac{2}{R_\mathrm{m}} = \frac{1}{R_1} + \frac{1}{R_2}. \tag{5}$$

We propose to extend this criterium to approaching walls of expanding bubbles. Because the radius and with it the approach velocity of oscillating bubbles change during a cycle, so does the Weber number. The approach velocity for expanding bubbles with a constant center-to-center distance is

$$u = \dot{R}_1 + \dot{R}_2\,. \tag{6}$$

If the Weber number is low (We$\lessapprox$0.5), bubble coalescence will always occur, without flattening of the adjacent surfaces prior to contact [17]. In the high Weber number regimen (We$\gtrapprox$1), coalescence is determined by a second step, after flattening: drainage of the interposed liquid film. When the expansion time is less than the time needed for film drainage, the bubbles will bounce off each other [23].

The radial velocity of the liquid in the film is a combination of a plug flow driven by the motion of the interfaces, and a laminar velocity profile (analogous to Poiseuille flow) driven by the radial pressure gradient [24], [25]. If the bubble surfaces consist of a high concentration of surfactant, on our working scales the interfaces are to be considered immobile (no-slip) [26]. In the case of no-slip interfaces, the interfacial tangential velocity is zero, so the plug flow contribution is zero [24]. In the case of free interfaces, the Poiseuille contribution to the drainage flow becomes negligible [26], [24]. The film drainage time for free radial surfaces is approximated by the equation [27], [28]:

$$\tau_\mathrm{d} \approx R_\mathrm{f} \sqrt{\frac{\rho}{8\,p}}\ \log\left(\frac{h_\mathrm{i}}{h_\mathrm{c}}\right)\,, \tag{7}$$

where R_f is the film radius, h_i is the initial thickness, h_c is the critical film thickness, at which the film ruptures, and p is the pressure difference between film and surrounding fluid which is taken

$$p = \sigma\left(\frac{1}{R_1} + \frac{1}{R_2}\right). \tag{8}$$

In our computations, we take

$$\begin{aligned} \rho &= 998\ \mathrm{kg\ m^{-3}}, \\ \sigma &= 0.072\ \mathrm{N\ m^{-1}},\ \text{and} \\ h_\mathrm{c} &= 10\ \mathrm{nm}\,. \end{aligned} \tag{9}$$

Flattening takes place when:

$$\dot{R}_1 + \dot{R}_2 \gg \frac{\mathrm{d}h}{\mathrm{d}t}, \tag{10}$$

whereas the flat film drainage happens in the next stage, when

$$\dot{R}_1 \approx \dot{R}_2 \approx 0. \tag{11}$$

Thus, during drainage, on our timescales, we may consider p and R_f constant over time [9].

Calculated drainage times from an inertial drainage model assuming clean, stress-free interfaces are consistent with the observations: For large (fully expanded) bubbles the drainage times are too large (larger than a bubble oscillation cycle) to allow for film drainage and coalescence (*cf.* Figure 5). Smaller microbubble fragments, however, easily coalesce on very short timescales [9], [22].

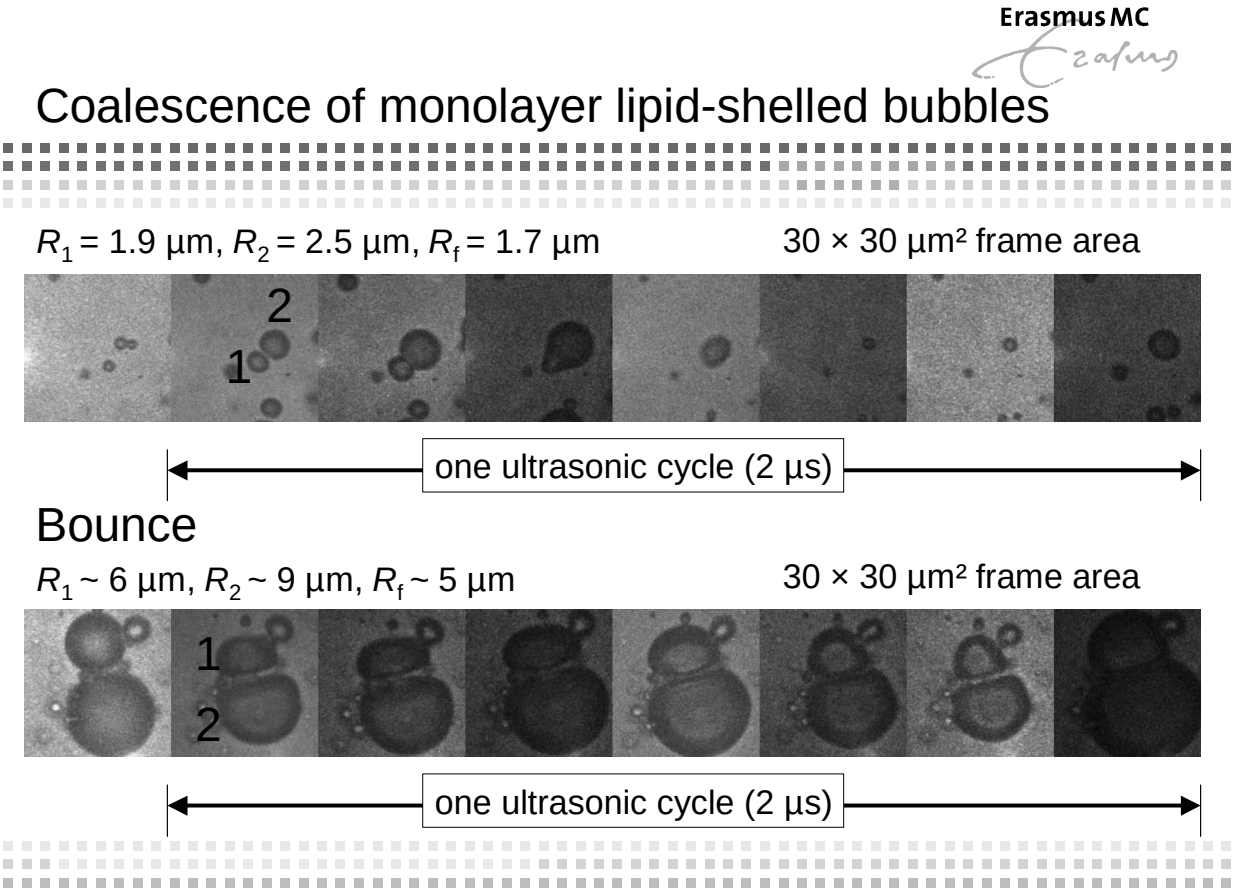

Fig. 5. Coalescing and bouncing Bracco microbubbles during expansion. Interframe times are 0.33 μs. Each frame corresponds to a $30 \times 30 \mu\text{m}^2$ area.

V. Conclusions

It takes tens of ultrasonic cycles to drive bubbles into each other, but it takes only one cycle to have them coalesce, if they are small enough. Despite the high approach velocity for large bubbles, drainage times are so high, that coalescence cannot occur. The total time of coalescence is approximated by the approach time added to the drainage time. If the Weber number is lower than 0.5, the drainage time itself is zero.

Ultrasound-induced coalescence of lipid-encapsulated Bracco contrast agent microbubbles is feasible. The coalescence of microbubbles might be used to increase the acoustic response from bulk agent at relatively low acoustic frequencies, without increasing the dosage. A theoretically simple way to increase scattering from contrast agent would be to induce bubble coalescence until the bubbles reach resonant sizes.

References

[1] K. Vokurka, "Comparison of Rayleigh's, Herring's, and Gilmore's models of gas bubbles," *Acustica*, vol. 59, pp. 214–219, 1986.
[2] N. de Jong, *Acoustic properties of ultrasound contrast agents*. Rotterdam: N de Jong, 1993.
[3] N. de Jong, R. Cornet, and C. T. Lancée, "Higher harmonics of vibrating gas-filled microspheres. Part one: simulations," *Ultrasonics*, vol. 32, no. 6, pp. 447–453, 1994.
[4] L. Hoff, "Acoustic properties of ultrasonic contrast agents," *Ultrasonics*, vol. 34, pp. 591–593, 1996.
[5] P. J. A. Frinking, *Ultrasound Contrast Agents: acoustic characterization and diagnostic imaging*. Rotterdam: PJA Frinking, 1999.
[6] J. M. Gorce, M. Arditi, and M. Schneider, "Influence of bubble size distribution on the echogenicity of ultrasound contrast agents: A study of SonoVue^{TM}," *Invest. Radiol.*, vol. 35, no. 11, pp. 661–671, 2000.
[7] M. Postema, A. Bouakaz, C. T. Chin, and N. de Jong, "Simulations and measurements of optical images of insonified ultrasound contrast microbubbles," *IEEE Trans. Ultrason., Ferroelect., Freq. Contr.*, vol. 50, no. 5, pp. 523–536, 2003.

[8] K. E. Morgan, J. S. Allen, P. A. Dayton, J. E. Chomas, A. L. Klibanov, and K. W. Ferrara, "Experimental and theoretical evaluation of microbubble behavior: Effect of transmitted phase and bubble size," *IEEE Trans. Ultrason., Ferroelect., Freq. Contr.*, vol. 47, no. 6, pp. 1494–1509, 2000.

[9] M. Postema, P. Marmottant, C. T. Lancée, S. Hilgenfeldt, and N. de Jong, "Ultrasound-induced microbubble coalescence," *Ultrasound Med. Biol.*, vol. in press, 2004.

[10] Z. Zhou and B. Joós, "Mechanisms of membrane rupture: from cracks to pores," *Phys. Rev. B*, vol. 56, no. 6, pp. 2997–3009, 1997.

[11] M. Postema, A. van Wamel, C. T. Lancée, and N. de Jong, "Ultrasound-induced encapsulated microbubble phenomena," *Ultrasound Med. Biol.*, vol. 30, no. 6, pp. 827–840, 2004.

[12] P. A. Dayton, K. E. Morgan, A. L. Klibanov, G. Brandenburger, K. R. Nightingale, and K. W. Ferrara, "A preliminary evaluation of the effects of primary and secondary radiation forces on acoustic contrast agents," *IEEE Trans. Ultrason., Ferroelect., Freq. Contr.*, vol. 44, no. 6, pp. 1264–1277, 1997.

[13] G. Marrucci, "A theory of coalescence," *Chem. Eng. Sci.*, vol. 24, pp. 975–985, 1969.

[14] D. S. Dimitrov and I. B. Ivanov, "Hydrodynamics of thin liquid films. On the rate of thinning of microscopic films with deformable interfaces," *J. Colloid. Interf. Sci.*, vol. 64, no. 1, pp. 97–106, 1978.

[15] I. B. Ivanov, D. S. Dimitrov, and B. P. Radoyev, "Generalized equations of thin films hydrodynamics and their application to the calculations of the thinning rate of films with non-deformed surfaces," *Kolloid. Zh.*, vol. 41, no. 1, pp. 36–42, 1979.

[16] C. Y. Lin and J. C. Slattery, "Thinning of a liquid film as a small drop or bubble approaches a fluid-fluid interface," *AIChE J.*, vol. 28, no. 5, pp. 786–792, 1982.

[17] A. K. Chesters and G. Hofman, "Bubble coalescence in pure liquids," *Appl. Sci. Res.*, vol. 38, pp. 353–361, 1982.

[18] P. C. Duineveld, *Bouncing and coalescence of two bubbles in water*. Enschede: PC Duineveld, 1994.

[19] M. Postema, A. Bouakaz, C. T. Chin, and N. de Jong, "Optically observed microbubble coalescence and collapse," *Proc. IEEE Ultrason. Symp.*, pp. 1900–1903, 2002.

[20] M. A. B. Postema, *Medical Bubbles*. Bergschenhoek: Michiel Postema, 2004.

[21] O. Reynolds, "On the theory of lubrication and its application to Mr. Beauchamp Tower's experiments, including an experimental determination of the viscosity of olive oil," *Philos. Trans. Roy. Soc. A*, vol. 177, pp. 157–234, 1886.

[22] M. Postema, P. Marmottant, C. T. Lancée, M. Versluis, S. Hilgenfeldt, and N. de Jong, "Ultrasound-induced coalescence of free gas microbubbles," *Proc. IEEE Ultrason. Symp.*, vol. in press, 2004.

[23] R. V. Chaudhari and H. Hofmann, "Coalescence of gas bubbles in liquids," *Rev. Chem. Eng.*, vol. 10, no. 2, pp. 131–190, 1994.

[24] E. Klaseboer, J. P. Chevaillier, C. Gourdon, and O. Masbernat, "Film drainage between colliding drops at constant approach velocity: experiments and modeling," *J. Colloid. Interf. Sci.*, vol. 229, pp. 274–285, 2000.

[25] D. F. Young, B. R. Munson, and T. H. Okiishi, *A Brief Introduction to Fluid Mechanics*, 2nd ed. New York: John Wiley & Sons, 2000.

[26] L. van Wijngaarden, "The mean rise velocity of pairwise-interacting bubbles in liquid," *J. Fluid Mech.*, vol. 251, pp. 55–78, 1993.

[27] R. D. Kirkpatrick and M. J. Lockett, "The influence of approach velocity on bubble coalescence," *Chem. Eng. Sci.*, vol. 29, pp. 2363–2373, 1974.

[28] L. Hagesæther, *Coalescence and break-up of drops and bubbles*. Trondheim: Norwegian University of Science and Technology, 2002.